



Rapgef2, a guanine nucleotide exchange factor for Rap1 small GTPases, plays a crucial role in adherence junction (AJ) formation in radial glial cells through ERK-mediated upregulation...

Farag, Maged Ibrahim

Yoshikawa, Yoko

Maeta, Kazuhiro

Kataoka, Tohru

(Citation)

Biochemical and Biophysical Research Communications, 493(1):139-145

(Issue Date)

2017-11-04

(Resource Type)

journal article

(Version)

Accepted Manuscript

(Rights)

©2017 Elsevier.

This manuscript version is made available under the CC-BY-NC-ND 4.0 license
<http://creativecommons.org/licenses/by-nc-nd/4.0/>

(URL)

<https://hdl.handle.net/20.500.14094/90004439>



Title: Rapgef2, a guanine nucleotide exchange factor for Rap1 small GTPases, plays a crucial role in adherence junction (AJ) formation in radial glial cells through ERK-mediated upregulation of the AJ-constituent protein expression

Authors: Maged Ibrahim Farag^{a, 1}, Yoko Yoshikawa^{a, 1}, Kazuhiro Maeta^{a, 2}, and Tohru Kataoka^{a, *}

Affiliations: ^aDivision of Molecular Biology, Department of Biochemistry and Molecular Biology, Kobe University Graduate School of Medicine, Kobe 650-0017, Japan.

***Corresponding author.** Address: Division of Molecular Biology, Department of Biochemistry and Molecular Biology, Kobe University Graduate School of Medicine, 7-5-1 Kusunoki-cho, Chuo-ku, Kobe 650-0017, Japan. Tel: +81-78-382-5380, Fax: +81-78-382-5399, E-mail address:

kataoka@people.kobe-u.ac.jp (T. Kataoka)

¹These authors contributed equally to this work.

²Present address: Department of Neurotherapeutics, Osaka University Graduate School of Medicine, 2-2 Yamadaoka, Suita 565-0871, Osaka, Japan

Keywords: Rap1, small GTPase, Rapgef2, radial glial cells, adherence junction, ERK

Abbreviations: adherens junction, AJ; radial glial cell, RGC; extracellular signal-regulated kinase, ERK; guanine nucleotide exchange factor, GEF; conditional knockout, cKO; ectopic cortical mass, ECM; embryonic day, E; brain lipid-binding protein, BLBP; mitogen-activated ERK kinase, MEK; c-jun N-terminal kinase, JNK; zonula occludens-1, ZO-1; 4',6-diamidino-2-phenylindole, DAPI; small interfering RNA, siRNA; quantitative reverse transcription-PCR, qRT-PCR.

Abstract

Rapgef2 and Rapgef6 define a subfamily of guanine nucleotide exchange factors for Rap1, characterized by possession of the Ras/Rap-associating domains and implicated in the etiology of schizophrenia. We previously found that dorsal telencephalon-specific *Rapgef2* conditional knockout mice exhibits severe defects in formation of apical surface adherence junctions (AJs) and localization of radial glial cells (RGCs). In this study, we analyze the underlying molecular mechanism by using primary cultures of RGCs established from the developing cerebral cortex. The results show that Rapgef2-deficient RGCs exhibit a decreased ability of neurosphere formation, morphological changes represented by regression of radial glial (RG) fibers and reduced expression of AJ-constituent proteins such as N-cadherin, zonula occludens-1, E-cadherin and β -catenin. Moreover, siRNA-mediated knockdown of Rapgef2 or Rap1A inhibits the AJ protein expression and RG fiber formation while overexpression of Rapgef2, Rapgef6, Rap1A^{G12V} or Rap1B^{G12V} in Rapgef2-deficient RGCs restores them. Furthermore, Rapgef2-deficient RGCs exhibit a reduction in phosphorylation of extracellular signal-regulated kinase (ERK) leading to downregulation of the expression of c-jun, which is implicated in the AJ protein expression. These results indicate a crucial role of the Rapgef2-Rap1A-ERK-c-jun pathway in regulation of the AJ formation in RGCs.

1. Introduction

Cerebral cortical development requires highly orchestrated events involving proliferation,

differentiation and migration of neural progenitors and neurons. During neurogenesis, RGCs, located in the ventricular zone at the apical side of the neuroepithelium, function as neural progenitors and generate self-renewing RGCs and neurons as well as committed intermediate progenitor cells [1]. Intermediate progenitor cells move to the subventricular zone, divide and differentiate into neurons. Newly-born neurons migrate to the intermediate zone, where they change their morphology from multipolar to bipolar and migrate along the RG fibers to the cortical plate. Finally, they undergo RG fiber-independent somal translocation to reach their final destinations.

Rap1 small GTPases, consisting of two isoforms Rap1A and Rap1B, play pivotal roles in regulation of cell proliferation, polarity, endocytosis and cell adhesion by cycling between GTP-bound active and GDP-bound inactive forms [2]. Interconversion between the two forms is reciprocally catalyzed by guanine nucleotide exchange factors (GEFs) and GTPase-activating proteins, where GEFs activate Rap1 in response to extracellular stimuli by catalyzing GDP release and thereby accelerating GTP loading. There exist more than ten GEFs specific for Rap1, including Rapgef1 to 6, which are regulated by distinct mechanisms and responsible for differential regulation of Rap1 activity in spacio-temporally defined and cell-type-specific manners [2]. During the cerebral cortical development, Rap1 plays crucial roles in neuronal migration, particularly in multipolar migration, multipolar-bipolar transition and terminal translocation but not RG fiber-guided locomotion [3-6]. In these cases, Rapgef1, also called C3G, is involved in Rap1 activation downstream of the Reelin signaling.

Rapgef2, also called RA-GEF-1 or PDZ-GEF1 [7-9], and Rapgef6, also called RA-GEF-2 [10],

constitute a unique Rap1-GEF subfamily characterized by possession of the Ras/Rap-associating domain and the PSD-95/DlgA/ZO-1 domain. Through association with the GTP-bound forms of Rap1 and M-Ras at the Ras/Rap-associating domains, they are recruited from the cytoplasm to the Golgi complex and the plasma membranes, respectively, and cause Rap1 activation by the action of their CDC25-homology domains [9]. We found that dorsal telencephalon-specific *Rapgef2* conditional knockout (*Rapgef2*-cKO) mice develop an ectopic cortical mass (ECM) resembling that seen in subcortical band heterotopia [10] and that additional knockout of *Rapgef6* in *Rapgef2*-cKO mice resulted in gross enlargement of the ECM [11] while knockout of *Rapgef6* alone had no discernible effect on the brain morphology [11-13]. Moreover, *Rapgef2*-cKO mice displayed severe defects in formation of the apical surface structure, which is composed of an assembly of the endfeet of the apical RG fibers linked together by an array of AJs, resulting in earlier detachment and aberrant localization of RGCs around embryonic day (E) 14.5 [11]. *Rap1*-cKO mice also exhibited almost identical phenotypes [14]. In addition, *Rapgef2* and Rap1 are implicated in multipolar-bipolar transition of post-mitotic neurons [5, 11, 14]. However, little is known about the molecular mechanism underlying these functions of *Rapgef2* and Rap1 during cortical development. In this study, we use a primary culture of RGCs established from the developing cerebral cortex to address this problem.

2. Materials and methods

2.1. Antibodies (Abs) and chemicals

Following primary Abs were used for indirect immunostaining and western blot analyses; rabbit Abs: anti-Rapgef2 [12], anti-Rapgef6 [13], anti-Rap1A (Abcam, ab197673), anti-Rap1B (Abcam, ab154756), anti-brain lipid-binding protein (BLBP) (Abcam, ab32423), anti-mitogen-activated ERK kinase (MEK) (CST, 9122S), anti-phospho-MEK (S217/221) (CST, 9121S), anti-ERK (CST, 9102S), anti-phospho-ERK (T202/Y204) (CST, 9101S), anti-c-jun N-terminal kinase (JNK) (CST, 9258S), anti-phospho-JNK (T183/Y185) (CST, 4668S), anti-phospho-c-jun (Ser63) (CST, 9261S) and anti-c-jun (CST, 9165S), and mouse Abs: anti-nestin (BD, 556309), anti- β -catenin (BD, 610153), anti-zonula occludens-1 (ZO-1) (Thermo Scientific, ZO1-1A12), anti-E-cadherin (Thermo Scientific, 4A2C7), anti-N-cadherin (BD, 610920), anti-afadin (Abcam, ab90809) and mouse anti- β -actin (Millipore, MAB1501R). Following secondary antibodies were used; donkey Abs: CF488A-anti-rabbit IgG (Biotium, 20015) and CF555-anti-rabbit IgG (Biotium, 20038), and goat Abs: CF488A-anti-mouse IgG (Biotium, 20018), CF555-anti-mouse IgG (Biotium, 20231) and horseradish peroxidase-conjugated anti-rabbit and anti-mouse IgGs (GE Healthcare). Trametinib, AGE 3482 and 4',6-diamidino-2-phenylindole (DAPI) were purchased from Selleckchem, Tocris and Thermo Scientific, respectively.

2.2. Animals and genotyping

Generation of *Rapgef2*^{flox/flox} (*Rapgef2*-f/f) and *Rapgef2*^{flox/flox}; *Emx1*^{Cre/+} (*Rapgef2*-cKO) mice were generated as described [10, 11]. Genotypes were determined by PCR using the primers P1 (5'-GTCAGACTAGCAGCAGACCACCTAG-3') and P4 (5'-CGAGTCCTGAACATAAGGGCAGGG-3')

as described previously [10] (Fig. 1A). The use and care of the animals were reviewed and approved by the Institutional Animal Care and Use Committee of Kobe University.

2.3. Neurosphere and RGC cultures

Cerebral cortices were dissected from brains isolated from *Rapgef2*-f/f and *Rapgef2*-cKO embryos at E14.5 as described [11] and dissociated by pipetting in Dulbecco's modified Eagle's medium (DMEM)/Hams F12 medium (Nacalai tesque). The resulting cell suspension was filtrated (40- μ m pore size) and 7.4×10^5 cells were transferred to a Φ 10-cm dish and cultured in DMEM/Hams F12 containing 2% B27 (Gibco), 200 mM L-glutamine (Gibco), 0.1% penicillin/streptomycin (Nacalai tesque), 20 ng/ml fibroblast growth factor b (Millipore) and 20 ng/ml epidermal growth factor (Gibco) at 37°C for 7 days to form neurospheres [15, 16]. Thereafter, the neurospheres were collected by centrifugation at 1,500 rpm for 5 min, dissociated by pipetting and cultured similarly to form neurospheres at passage 1. This procedure was repeated to form neurosphere cultures at passage n , from which RGC cultures at passage $n+1$ were derived by spreading the dissociated neurospheres on Φ 6-cm dishes or 4-chamber slide glasses coated with 50 μ g/ml poly-L-lysine (Sigma) and 3 μ g/ml laminin (Gibco).

2.4. Transfection of RGCs by small interfering RNAs (siRNAs) and expression plasmids

RGCs were transfected with an siRNA targeting *Rapgef2* (5'-auaacuucugcccacuuccaucgg-3'), *Rapgef6* (5'-uaauuuuaaguccucaggaguccg-3'), *Rap1A* (5'-aaggacuacuagcuuguacucacgc-3') or *Rap1B*

(5'-gacaguggaacaacugugcauucuu-3') by using RNAiMAX Lipofectamin (Invitrogen) according to the manufacturer's instruction. Also, they were transfected with pFlag-CMV2-Rapgef2 [9], pFlag-CMV2-Rapgef6 [9], pEF-BOS-HA-Rap1A^{G12V} [8], pEF-BOS-HA-Rap1B^{G12V} [8] or pFlag-CMV2 (Sigma) by using Lipofectamin 2000 (Invitrogen). Thereafter, the cells were incubated for 72 h at 37°C and subjected to further experiments.

2.5. Immunostaining and western immunoblotting

RGCs, grown to 50% confluency, were fixed, permeabilized and immunostained as described previously [11]. Neurospheres and RGCs in culture were solubilized, separated by SDS-PAGE and subjected to immunoblotting as described previously [13]. A representative result was shown when the experiment performed at least three times gave equivalent results.

2.6. RNA isolation and quantitative reverse transcription-PCR (qRT-PCR)

Total RNAs were isolated from neurospheres and RGCs by using TRIzol (Thermo Scientific). SYBR Premix Ex Taq II Kit (Takara Bio) was used to carry out qRT-PCR with Thermal Cycler Dice Real Time System (Takara Bio). Relative mRNA levels were determined by the comparative *Ct* method, followed by normalization with the *β-actin* mRNA level. Primers used are listed in supplementary Table 1.

2.7. Statistical analyses

The data were presented as the mean \pm SEM. Statistical significance for groups of three or more was determined by student's *t-test*. Differences were considered to be statistically significant when the *p* value was less than 0.05. *, *p*<0.05; **, *p*<0.01; and ***, *p*<0.001.

3. Results

3.1. Morphological and adherent properties of RGCs deficient in *Rapgef2*

E14.5 embryos were collected from pregnant mice generated by mating *Rapgef2*-f/f mice with *Rapgef2*^{fllox/+};*Emx1*^{Cre/+} mice as described before [10, 11]. Cerebral cortices were dissected from their brains, and genomic DNAs were isolated from their small portions and subjected to genotyping by PCR using the primers P1 and P4, which was expected to yield 1.1-kb and 0.6-kb products for the *Rapgef2*^{fllox} and *Rapgef2*-targeted alleles, respectively (Fig. 1A). Very efficient targeting was achieved in *Rapgef2*-cKO cerebral cortex (10, 11). We established neurosphere cultures from the cerebral cortices of E14.5 *Rapgef2*-f/f and *Rapgef2*-cKO embryos. PCR analyses using P1 and P4 showed that neurospheres derived from *Rapgef2*-cKO cortices predominantly yielded the 0.6-kb product, confirming the high efficiency of targeting (Fig. 1A). Next, RGC cultures were established by dissociating the neurospheres and spreading the dissociated cells onto the adherent surface of laminin/lysine-coated culture dishes. We found that successive passages of RGC cultures resulted in accumulation of more adherent *Rapgef2*-f/f cells over *Rapgef2*-deficient cells. We therefore conducted successive passages as neurosphere cultures and succeeded in preventing the *Rapgef2*-f/f cell accumulation. The passage-4 neurospheres were

dissociated and each half was used to establish a neurosphere culture or a RGC culture at passage 5. Genotyping showed that *Rapgef2*-targeted cells occupied a major population in both of the cultures (Fig. 1B). This was also evidenced by substantially reduced expression of the *Rapgef2* mRNA in the *Rapgef2*-cKO cultures, where the proportion of *Rapgef2*-f/f cells was roughly estimated to be 12% and 18% for the neurosphere and RGC cultures, respectively (Fig. 1C). Because RGC culture cells retained high expression of developmental markers for RGCs, such as BLBP and nestin (Fig. S1), they were regarded as the equivalents of RGCs and hereafter called “RGCs” in culture.

Comparison between the *Rapgef2*-f/f and *Rapgef2*-cKO neurosphere cultures revealed that *Rapgef2*-cKO neurospheres were much smaller in size than *Rapgef2*-f/f neurospheres: neurospheres with a diameter over 100 μm were almost nonexistent in *Rapgef2*-cKO cultures (Fig. 1D). This suggested that *Rapgef2*-deficient cells had lower adherent capacity. Moreover, comparison of the morphology of RGCs between the *Rapgef2*-f/f and *Rapgef2*-cKO cultures revealed that *Rapgef2*-cKO RGCs had their RG fibers markedly shortened or almost disappeared compared to *Rapgef2*-f/f RGCs (Fig. 1E, Fig. S1). Because demarcation of the cell bodies and RG fibers was difficult, the total cell lengths were measured. In the *Rapgef2*-cKO RGC culture, cells with the lengths longer than 50 μm were scarcely observed and a majority of cells totally lost the RG fibers. Moreover, *Rapgef2*-cKO RGCs assumed more round morphology with a smaller size (Fig. S1).

3.2. Reduction of the AJ protein expression in RGCs deficient in *Rapgef2*

To clarify the molecular mechanism underlying the disruption of the apical surface AJ structures in *Rapgef2*-cKO cerebral cortex, we compared the expression levels of AJ-constituent proteins such as N-cadherin, ZO-1, E-cadherin, β -catenin and afadin, which were heavily concentrated on the apical surface structure, between *Rapgef2*-f/f and *Rapgef2*-cKO RGCs. The results showed that the expression of N-cadherin, ZO-1, E-cadherin and β -catenin, but not afadin, was substantially diminished in *Rapgef2*-cKO RGCs at both the mRNA and protein levels (Fig. 2A and B) and also in *Rapgef2*-cKO neurospheres (Fig. S2). Moreover, immunostaining for the AJ proteins showed that while all *Rapgef2*-f/f RGCs were positive for N-cadherin, ZO-1, E-cadherin and β -catenin as well as *Rapgef2*, most of *Rapgef2*-cKO RGCs, negative for *Rapgef2*, were stained very weakly for N-cadherin, ZO-1, E-cadherin and β -catenin (Fig. 2C-F). A minor population of *Rapgef2*-cKO RGCs, which were all positive for *Rapgef2*, N-cadherin, ZO-1, E-cadherin and β -catenin, were likely to correspond to *Rapgef2*-f/f cells.

3.3. Effects of knockdown and overexpression of *Rapgef2*, *Rapgef6* and *Rap1* on AJ protein expression

We examined the effects of siRNA-mediated knockdown of *Rapgef2*, *Rapgef6*, *Rap1A* and *Rap1B* on the AJ protein expression in *Rapgef2*-f/f RGCs. Transfection of the *Rapgef2* siRNA yielded a substantial population of cells that showed very low expression of both *Rapgef2* and N-cadherin, indicating that *Rapgef2* knockdown inhibited the N-cadherin expression (Fig. 3A and B). Moreover, these cells assumed more round morphology and possessed shortened RG fibers compared to the cells expressing both *Rapgef2* and N-cadherin. Furthermore, *Rapgef2* knockdown also inhibited the expression of ZO-1,

E-cadherin and β -catenin (Fig. S3A). We obtained similar results with *Rapgef2*-f/f RGCs transfected with the *Rap1A* siRNA (Fig. 3B, Fig. S3A). On the contrary, the *Rapgef6* and *Rap1B* siRNAs failed to inhibit the AJ protein expression and alter the cell morphology.

Next we examined the effects of overexpression of *Rapgef2*, *Rapgef6* and the constitutively activated *Rap1* mutants, *Rap1A*^{G12V} and *Rap1B*^{G12V}, on the AJ protein expression in *Rapgef2*-cKO RGCs. Transfection of the expression plasmids for *Rapgef2*, *Rapgef6* and *Rap1A*^{G12V} all yielded substantial populations of cells that expressed N-cadherin, ZO-1, E-cadherin and β -catenin simultaneously with *Rapgef2*, *Rapgef6* and *Rap1A*^{G12V}, respectively (Fig. 3C and D, Fig. S3B). Moreover, these cells assumed less round morphology and resumed long RG fibers, which were similar to those of *Rapgef2*-f/f RGCs. On the other hand, upon transfection with the *Rap1B*^{G12V} expression vector, significant proportions of cells overexpressing *Rap1B*^{G12V} failed to show expression of the AJ proteins.

3.4. Roles of ERK and c-jun in *Rapgef2*/*Rap1A*-dependent regulation of AJ protein expression

Rap1 had been known to activate the Raf-MEK-ERK pathway through direct association with B-Raf in neurons [17, 18]. This led us to examine the role of this pathway in *Rapgef2*/*Rap1A*-dependent regulation of AJ protein expression. We found that the phosphorylation levels of MEK and ERK were substantially diminished in *Rapgef2*-cKO RGCs compared to *Rapgef2*-f/f RGCs (Fig. 4A). Moreover, both the amounts of total and phosphorylated c-jun, a subunit of AP-1 transcription factor, were also diminished in *Rapgef2*-cKO RGCs. The activity of c-jun seemed to be regulated at the transcriptional

level because the *c-jun* mRNA level was also reduced (Fig. 4B) and because the phosphorylation level of JNK showed no change in *Rapgef2*-cKO RGCs (Fig. S4A). This result was consistent with the previous observation that c-jun expression is regulated by ERK phosphorylation [19, 20]. We next examined the role of the MEK-ERK-c-jun pathway in regulation of the AJ protein expression. Treatment of *Rapgef2*-f/f RGCs with Trametinib, a MEK inhibitor, inhibited the expression of not only c-jun but also N-cadherin, ZO-1, E-cadherin and β -catenin at both the mRNA and protein levels (Fig. 4C, Fig. S4B). Also, treatment with AGE3482, an inhibitor of c-jun phosphorylation, inhibited the expression of the AJ proteins but not c-jun at both the mRNA and protein levels.

4. Discussion

Rap1 was shown to play pivotal roles not only in integrin-mediated cell adhesion by transmitting “inside-out” signaling for integrin activation but also in cadherin-mediated cell adhesion by controlling the assembly of the AJ complex [19]. In this study, we have analyzed the molecular mechanism underlying the disruption of the apical surface AJs observed in developing *Rapgef2*-cKO cerebral cortex using primary cultures of RGCs isolated from E14.5 embryos and demonstrated a novel role of the *Rapgef2*-Rap1A-ERK-c-jun pathway in regulation of the expression of AJ proteins, such as N-cadherin, ZO-1, E-cadherin and β -catenin, in RGCs as illustrated in Fig. 4D. Also, *Rapgef2*-deficient RGCs exhibit a decreased ability to form neurospheres in culture, suggesting an impairment of their adherent

capacity. Because the AJ-constituent proteins are highly concentrated in the apical surface structure, downregulation of their expression observed in *Rapgef2*-deficient RGCs may well account for the disruption of the apical surface structure observed in *Rapgef2*-cKO cerebral cortex although we cannot exclude the possibility that another mechanism concerning the control of AJ complex assembly is also involved. Although the expression of afadin, also a key constituent of the AJs, is not affected in *Rapgef2*-cKO RGCs, *Rapgef2*/Rap1 may also contribute to the AJ formation through regulation of the afadin activity, which is regulated by direct association with GTP-bound Rap1 [20]. Moreover, we have shown that, compared to *Rapgef2*-f/f RGCs, *Rapgef2*-deficient RGCs in culture assume more round morphology with a smaller size and have their RG fibers markedly shortened or almost disappeared, both of which are partly reversed by overexpression of *Rapgef2* and *Rap1A*^{G12V}. These morphological alterations appear to bear a considerable resemblance to those observed *in vivo* for *Rapgef2*-cKO RGCs prematurely detached from the apical surface structure, which assume a round morphology and have their basal RG fibers heavily disorganized and their apical RG fibers disappeared [11].

Our results have also revealed that *Rapgef6* plays only an auxiliary role in the physiological condition although it possesses a redundant function with *Rapgef2* and is able to implement the *Rapgef2* function when artificially overexpressed. This is consistent with our previous observation that additional knockout of *Rapgef6* in *Rapgef2*-cKO mice results in gross enlargement of the ECM while knockout of *Rapgef6* alone has no discernible effect on the brain morphology [11-13]. On the other hand, *Rap1B* seems to have weaker activity to complement the *Rap1A* function.

We have also shown that the Rapgef2-Rap1A-ERK pathway regulates the AJ protein expression through upregulating c-jun expression in RGCs. This is consistent with the previous observations that the expression of N-cadherin and ZO-1 was upregulated by phosphorylations of ERK and c-jun [21-23]. However, the molecular mechanisms for transcriptional regulations of the expression of c-jun by activated ERK and of N-cadherin, ZO-1, E-cadherin and β -catenin by c-jun are presently unknown and remain to be clarified in our future studies. It is noteworthy that rare inherited copy number variations of the *RAPGEF2* and *RAPGEF6* genes were reported to exhibit strong genetic association with schizophrenia [24, 25]. Recent study showed that *Rapgef6*-knockout mice exhibited impaired function of the amygdala and hippocampus, brain regions implicated in schizophrenia pathophysiology [13]. Further investigation on the functions of Rapgef2 and Rapgef6 may advance our understanding of the mechanism of the cerebral corticogenesis as well as the etiology of various central nervous system diseases.

Acknowledgements

We thank all the members of our laboratory, especially Dr. Hironori Edamatsu, for valuable discussions.

Funding

This work was supported by JSPS KAKENHI Grant Number 20390080.

References

- [1] A. Hoerder-Suabedissen, Z. Molnár, Development, evolution and pathology of neocortical subplate neurons, *Nat. Rev. Neurosci.* 16 (2015) 133-146.
- [2] M. Gloerich, J. L. Bos, Regulating Rap small G-proteins in time and space. *Trends Cell Biol.* 21 (2011) 615-623.
- [3] A. K. Voss, J. M. Britto, M. P. Dixon, et al., C3G regulates cortical neuron migration, preplate splitting and radial glial cell attachment, *Development* 135 (2008) 2139-2149.
- [4] Y. Jossin, J. A. Cooper, Reelin, Rap1 and N-cadherin orient the migration of multipolar neurons in the developing neocortex, *Nat. Neurosci.* 14 (2011) 697-703.
- [5] T. Ye, J. P. Ip, A. K. Fu, et al., Cdk5-mediated phosphorylation of RapGEF2 controls neuronal migration in the developing cerebral cortex, *Nat. Commun.* 5 (2014) 4826.
- [6] S. J. Franco, I. Martinez-Garay, C. Gil-Sanz, et al., Reelin regulates cadherin function via Dab1/Rap1 to control neuronal migration and lamination in the neocortex, *Neuron* 69 (2011) 482-497.
- [7] J. de Rooij, N. M. Boenink, M. van Triest, et al., PDZ-GEF1, a guanine nucleotide exchange factor specific for Rap1 and Rap2, *J. Biol. Chem.* 274 (1999) 38125-38130.
- [8] Y. Liao, K. Kariya, C. D. Hu, et al., RA-GEF, a novel Rap1A guanine nucleotide exchange factor containing a Ras/Rap1A-associating domain, is conserved between nematode and humans, *J. Biol. Chem.* 274 (1999) 37815-37820.

- [9] X. Gao, T. Satoh, Y. Liao, et al., Identification and characterization of RA-GEF-2, a Rap guanine nucleotide exchange factor that serves as a downstream target of M-Ras, *J. Biol. Chem.* 276 (2001) 42219-42225.
- [10] S. E. Bilasy, T. Satoh, S. Ueda, et al., Dorsal telencephalon-specific RA-GEF-1 knockout mice develop heterotopic cortical mass and commissural fiber defect, *Eur. J. Neurosci.* 29 (2009) 1994-2008.
- [11] K. Maeta, H. Edamatsu, K. Nishihara, et al., Crucial role of Rapgef2 and Rapgef6, a family of guanine nucleotide exchange factors for Rap1 small GTPase, in formation of apical surface adherens junctions and neural progenitor development in the mouse cerebral cortex, *eNeuro* 3 (2016) e0142-16.
- [12] Y. Yoshikawa, T. Satoh, T. Tamura., et al., The M-Ras-RA-GEF-2-Rap1 pathway mediates tumor necrosis factor-alpha dependent regulation of integrin activation in splenocytes, *Mol. Biol. Cell* 18 (2007) 2949-2959.
- [13] R. J. Levy, M. Kvajo, Y. Li, et al., Deletion of Rapgef6, a candidate schizophrenia susceptibility gene, disrupts amygdala function in mice. *Transl. Psychiatry* 5 (2015) e577.
- [14] B. Shah, D. Lutter, Y. Tsytsyura, et al., Rap1 GTPases are master regulators of neural cell polarity in the developing neocortex, *Cereb. Cortex* 27 (2017) 1253-1269.
- [15] J. Stipursky, D. Francis, R. S. Dezone, et al., TGF-1 promotes cerebral cortex radial glia-astrocyte differentiation *in vivo*, *Front. Cell. Neurosci.* (2014), Article 393.
- [16] H. Azari, S. Sharififar, M. Rahman, et al., Establishing embryonic mouse neural stem cell culture using the neurosphere assay, *JoVE* (2011) 47.

- [17] A. C. Emery, M. V. Eiden, T. Mustafa, et al., Rapgef2 connects GPCR-mediated cAMP signals to ERK activation in neuronal and endocrine cells, *Sci. Signal.* 6 (2013) 281: ra51.
- [18] S. Hisata, T. Sakisaka, T. Baba, et al., Rap1-PDZ-GEF1 interacts with a neurotrophin receptor at late endosomes, leading to sustained activation of Rap1 and ERK and neurite outgrowth, *J. Cell Biol.* 178 (2007) 843-860.
- [19] B. Boettner, L. Van Aelst, Control of cell adhesion dynamics by Rap1 signaling, *Curr. Opin. Cell Biol.* 21 (2009) 684-693.
- [20] T. Hoshino, T. Sakisaka, T. Baba, et al., Regulation of E-cadherin endocytosis by nectin through afadin, Rap1, and p120ctn, *J. Biol. Chem.* 280 (2005) 24095-24103.
- [21] M. J. Marinissen, M. Chiariello, M. Pallante, et al., A network of mitogen-activated protein kinases links G protein-coupled receptors to the c-jun promoter: a role for c-Jun NH₂-terminal kinase, p38s, and extracellular signal-regulated kinase, *Mol. Cell. Biol.* 19 (1999) 4289-4301.
- [22] P. Lopez-Bergami, C. Huang, J. S. Goydos, et al., Rewired ERK-JNK signaling pathways in melanoma, *Cancer Cell* 11 (2007) 447-460.
- [23] Y. Shintani, M. A. Hollingsworth, M. J. Wheelock, et al., Collagen I promotes metastasis in pancreatic cancer by activating c-Jun NH₂-terminal kinase 1 and up-regulating N-cadherin expression, *Cancer Res.* 66 (2006) 11745-1153.
- [24] B. Xu, J. L. Roos, S. Levy, et al., Strong association of de novo copy number mutations with sporadic schizophrenia, *Nat. Genet.* 40 (2008) 880-885.

[25] B. Xu, A. Woodroffe, L. Rodriguez-Murillo, et al., Elucidating the genetic architecture of familial schizophrenia using rare copy number variant and linkage scans, *Proc. Natl. Acad. Sci. USA.* 106 (2009) 16746-16751.

Legends to Figures

Fig. 1. Morphology and neurosphere formation of Rapgef2-deficient RGCs. (A) Shown are the structures of the *Rapgef2*^{fllox} and *Rapgef2*-targeted alleles, on which the exons with their numbers and the loxP sites are shown by filled rectangles and triangles, respectively. Locations of the PCR primers P1 and P4 are indicated. The results of PCR genotyping of neurosphere cultures established from the cerebral cortices of two individual E14.5 *Rapgef2*-f/f (f/f) or *Rapgef2*-cKO (cKO) embryos are shown in the lower panel. (B) Passage-5 neurosphere and RGC cultures derived from the neurosphere cultures described in (A) were subjected to genotyping by PCR. (C) The *Rapgef2* mRNA levels of the neurosphere and RGC cultures described in (B) were quantitated by qRT-PCR. The data represented the mean \pm SEM of the results of 4 independent experiments, each conducted in triplicate. (D) Shown are representative phase contrast images of the neurosphere cultures described in (B). The percentages of neurospheres possessing the indicated diameters were determined by measuring more than 300 neurospheres (*right panel*). (E) Shown are representative phase contrast images of the RGC cultures described in (B). The total cell lengths of more than 280 cells were measured and classified as indicated (*right panel*).

Fig. 2. Reduction of the AJ protein expression in Rapgef2-deficient RGCs. (A) The mRNA levels of the indicated AJ proteins in the passage-5 RGC cultures described in Fig. 1B were quantitated by qRT-PCR. The data represented the mean \pm SEM of the results of 4 independent experiments, each conducted in

triplicate. (B) Lysates of the RGC cultures described in (A) were subjected to the detection of the indicated proteins by western immunoblotting with the respective Abs. The numbers below the lanes indicate the relative band intensities of the respective proteins normalized by those of β -actin. (C)-(F) The RGC cultures described in (A) were subjected to double immunofluorescence staining with the anti-Rapgef2 Ab (*red*) and either of the anti-N-cadherin (C), anti-ZO-1 (D), anti-E-cadherin (E) or anti- β -catenin (F) Ab (*green*). Nuclei were stained by DAPI (*blue*). The number in the inset shows the number of the positively stained cells in each panel.

Fig. 3. Effects of knockdown and overexpression of Rapgef2, Rapgef6 and Rap1 on AJ protein expression. (A) The mRNA levels of the indicated proteins in passage-5 *Rapgef2*-f/f RGCs transfected with the respective siRNAs or the corresponding scramble RNAs were quantitated by qRT-PCR. The data represented the mean \pm SEM of the results of 3 independent experiments, each conducted in quadruplicate. (B) The *Rapgef2*-f/f RGC cultures described in (A) were subjected to double immunofluorescence staining with the anti-Rapgef2 Ab (*red*) and the anti-N-cadherin Ab (*green*). Nuclei were stained by DAPI (*blue*). White arrowheads indicate cells in which expression of the respective protein was substantially reduced compared to the scramble RNA-transfected cells. (C) Passage-5 *Rapgef2*-cKO RGCs transfected with the expression plasmid for Rapgef2, Rapgef6, Rap1A^{G12V} or Rap1B^{G12V} or the empty vector were subjected to the measurements of the respective mRNA levels by qRT-PCR. The data represented the mean \pm SEM of the results of 3 independent

experiments, each conducted in quadruplicate. (D) The *Rapgef2*-cKO RGC cultures described in (C) were subjected to double immunofluorescence staining as described in (B). White arrowheads indicate cells which showed higher expression of the respective protein compared to the vector-transfected cells. Yellow arrowheads indicate cells which failed to show higher expression of N-cadherin while overexpressing Rap1B.

Fig. 4. Roles of ERK and c-jun in *Rapgef2*/Rap1A-dependent regulation of AJ protein expression. (A) Lysates of the RGC cultures described in Fig. 2A were subjected to the detection of the indicated proteins by western immunoblotting with the respective Abs. The numbers below the lanes indicate the relative band intensities of the respective proteins normalized by those of β -actin. (B) The *c-jun* mRNA levels in RGCs described in (A) were quantitated by qRT-PCR. The data represented the mean \pm SEM of the results of 3 independent experiments, each conducted in quadruplicate. (C) Lysates of the *Rapgef2*-f/f RGC cultures treated with DMSO (D), 10 μ M Trametinib (T) or 40 μ M AGE3482 (A) were subjected to the detection of the indicated proteins by western immunoblotting with the respective Abs. The numbers below the lanes indicate the relative band intensities of the respective proteins normalized by those of β -actin. (D) A model for the regulation of the AJ protein expression by the *Rapgef2*-Rap1A-ERK-c-jun signaling pathway is shown.

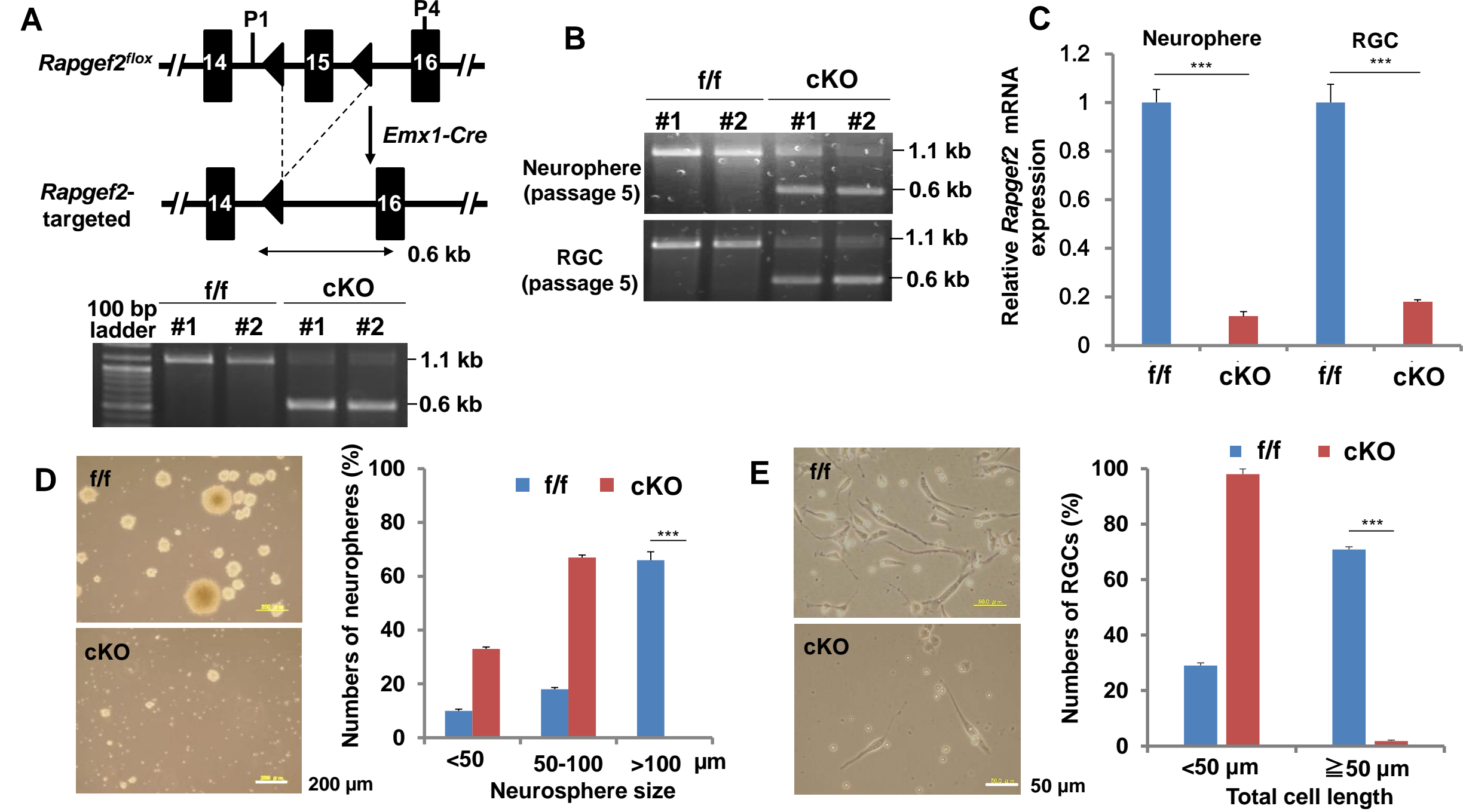
Fig. 1

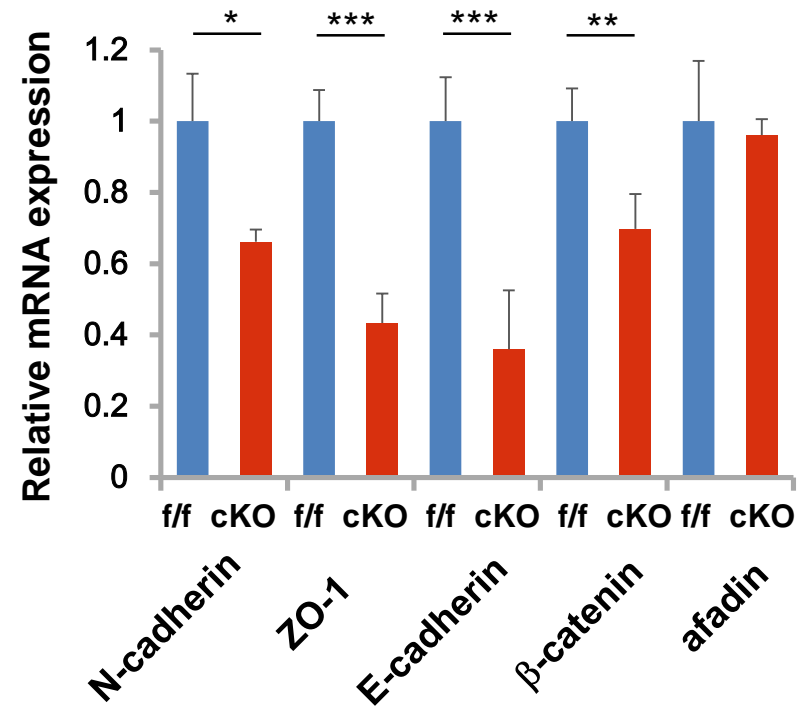
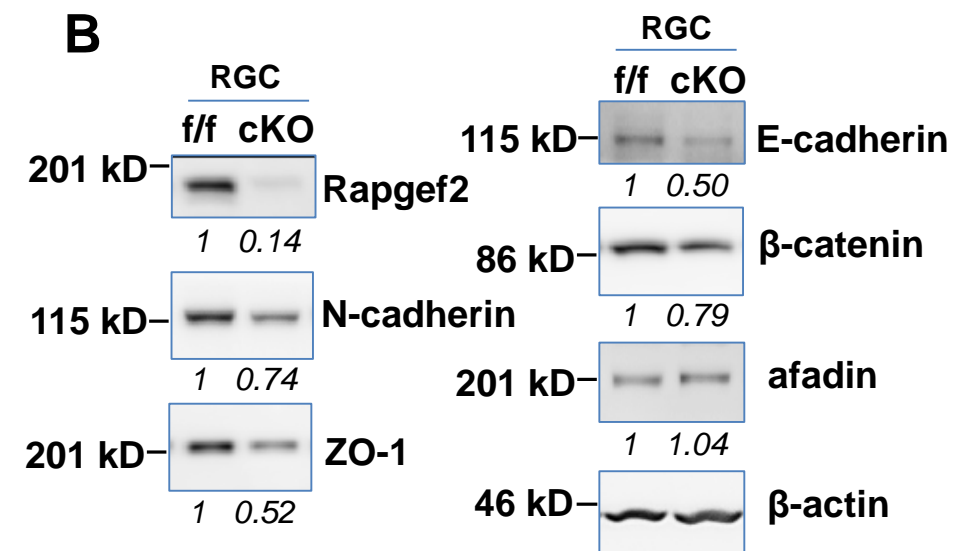
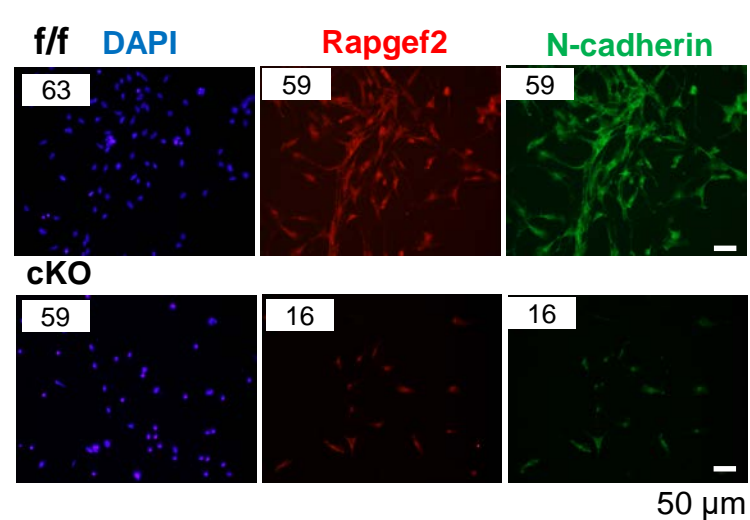
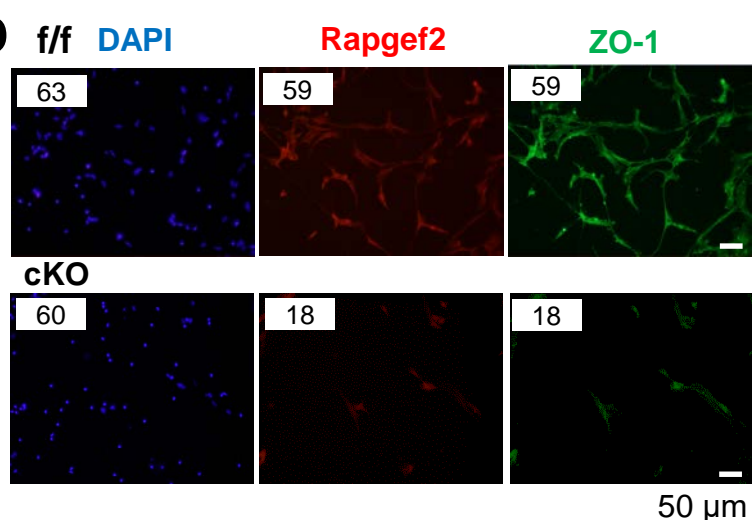
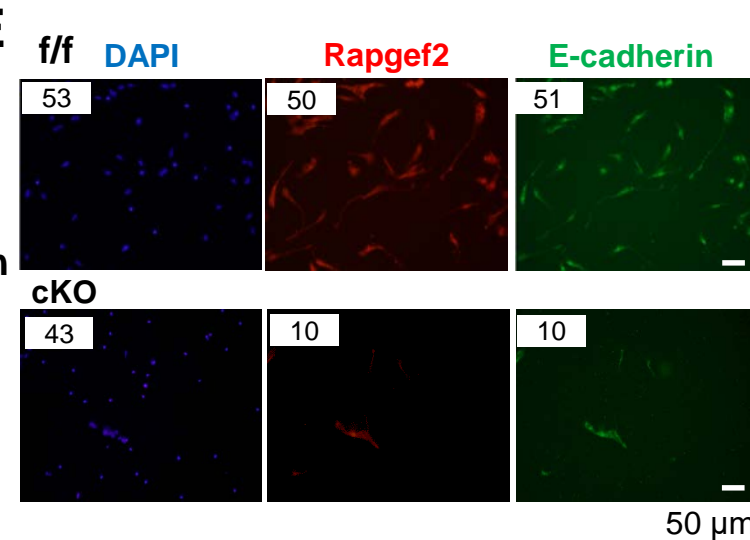
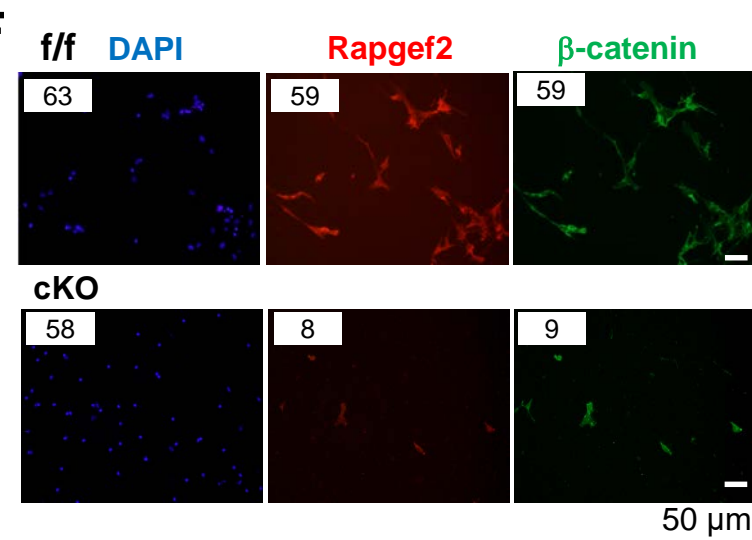
Fig. 2**A****B****C****D****E****F**

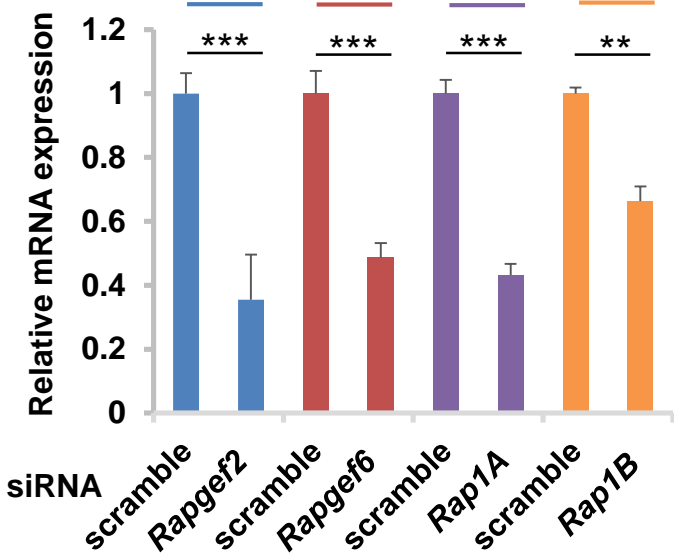
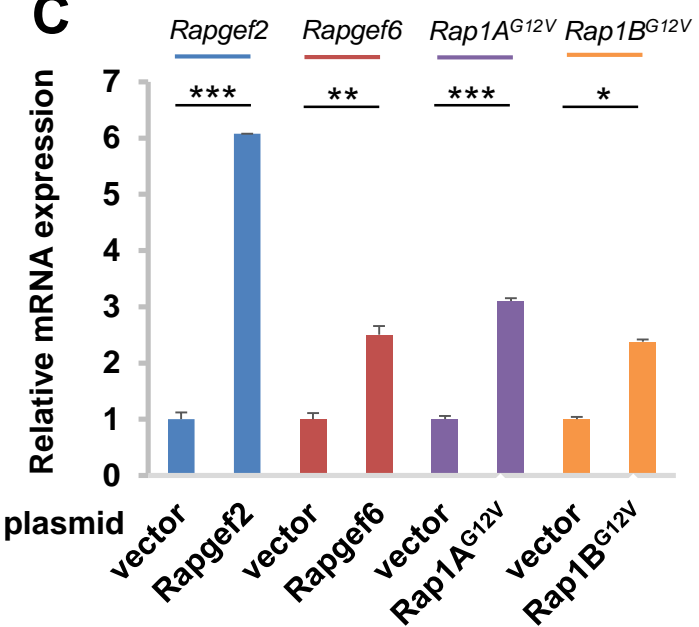
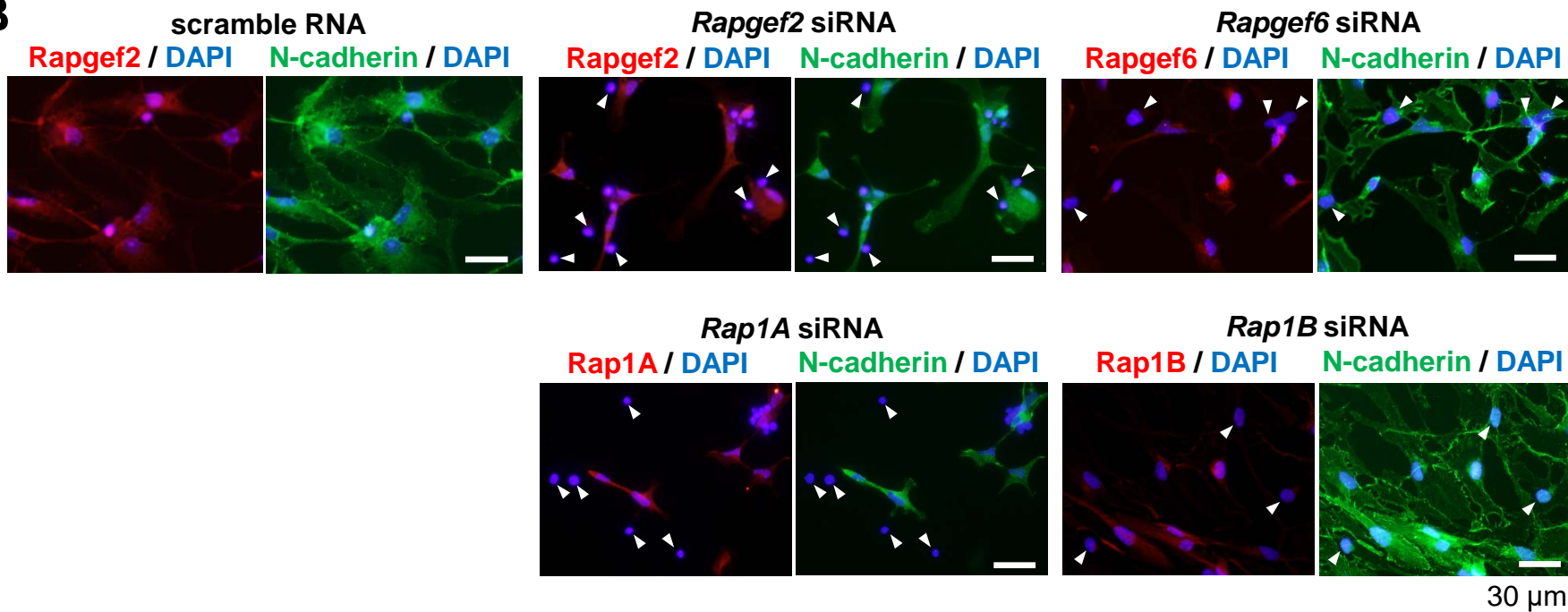
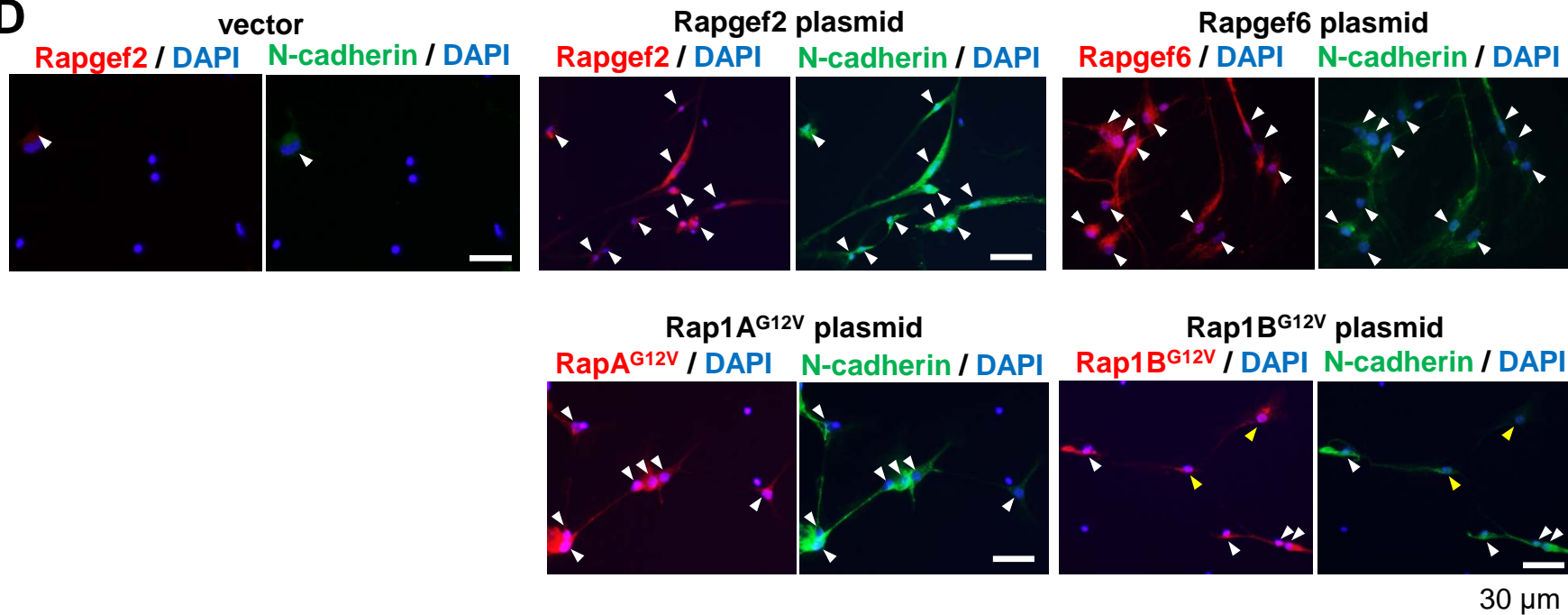
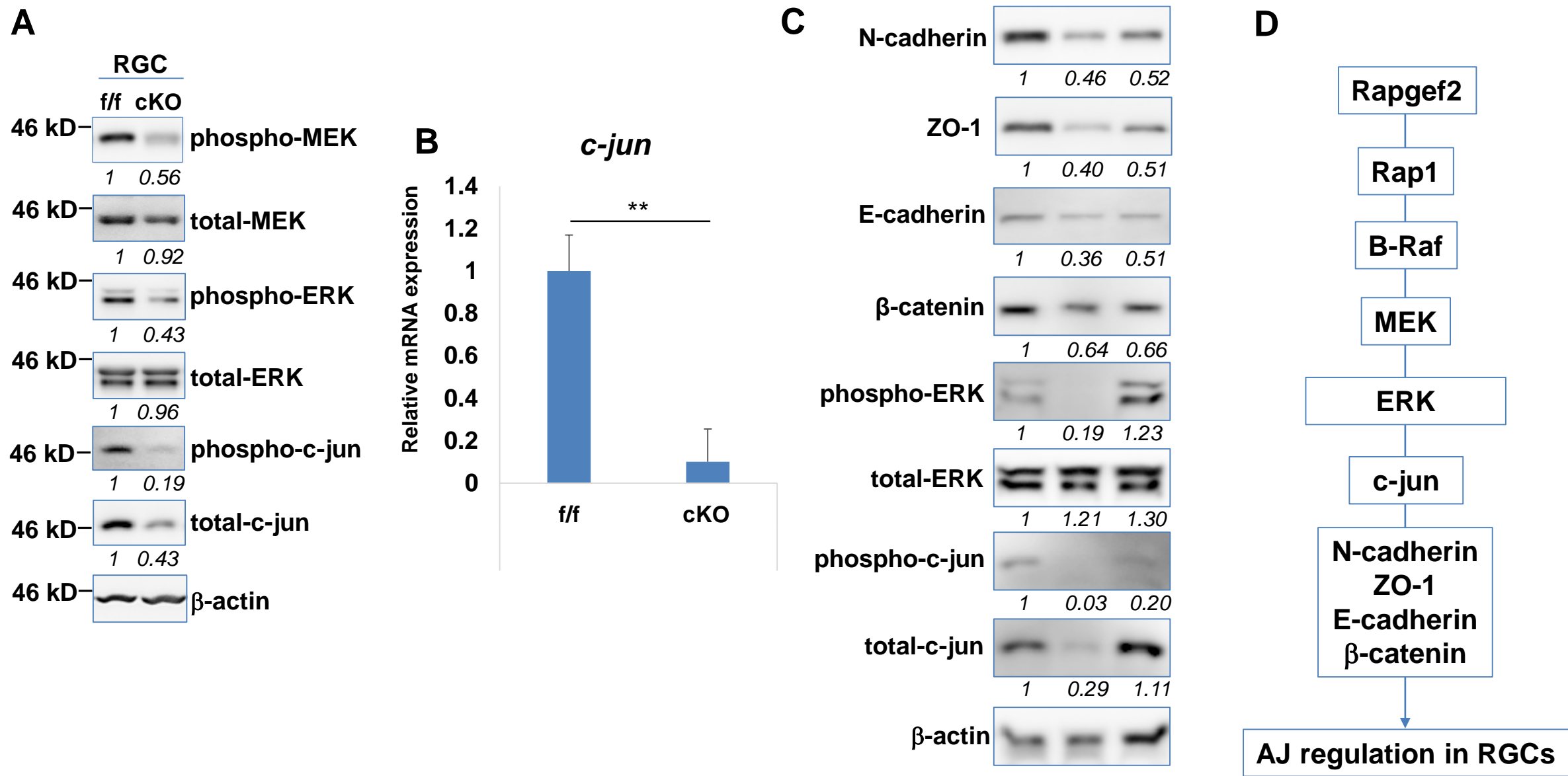
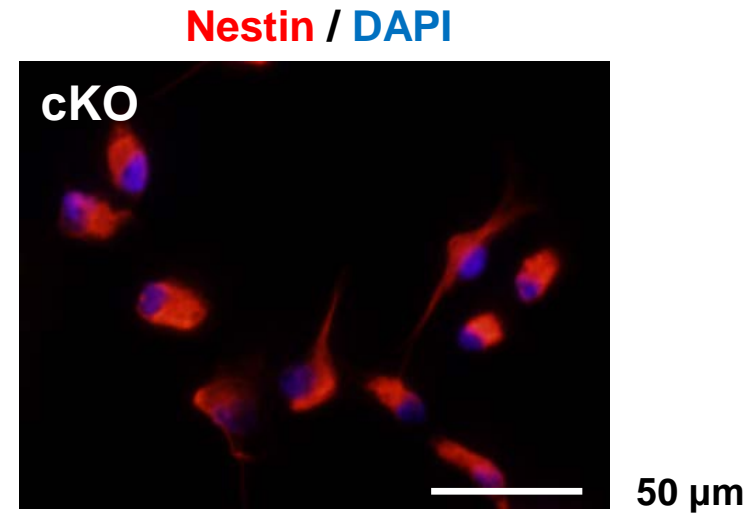
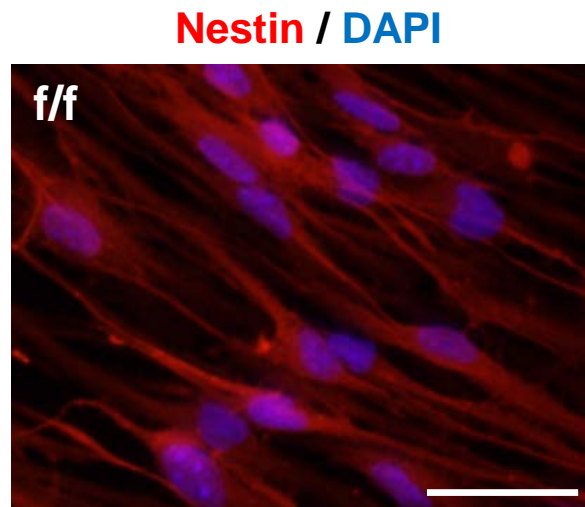
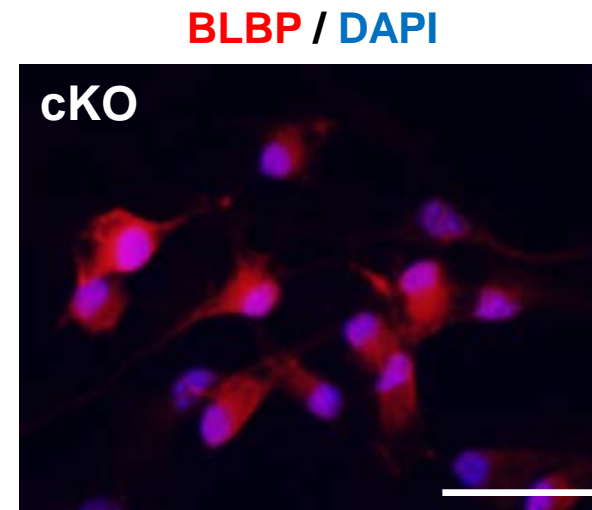
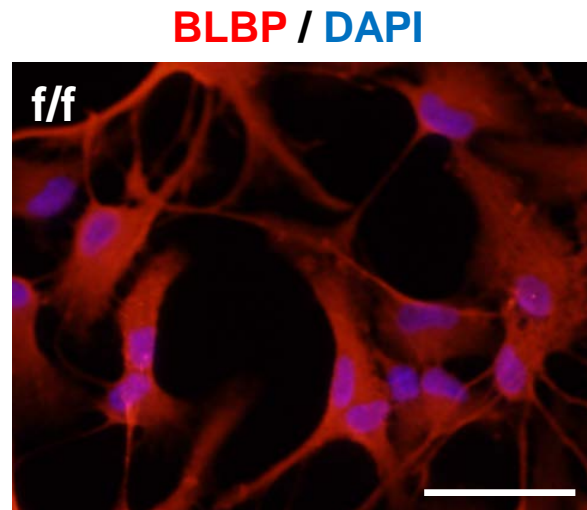
Fig. 3**A****C****B****D**

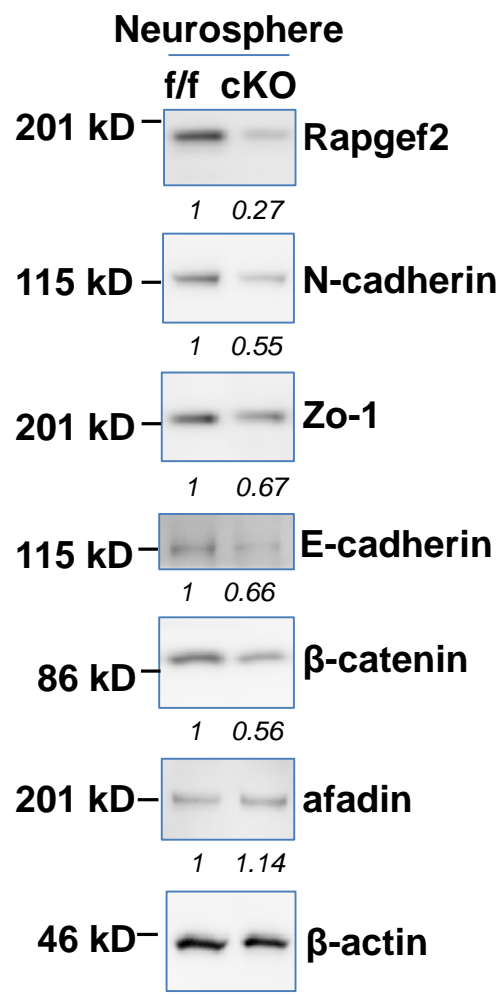
Fig. 4



Supplementary Figure 1

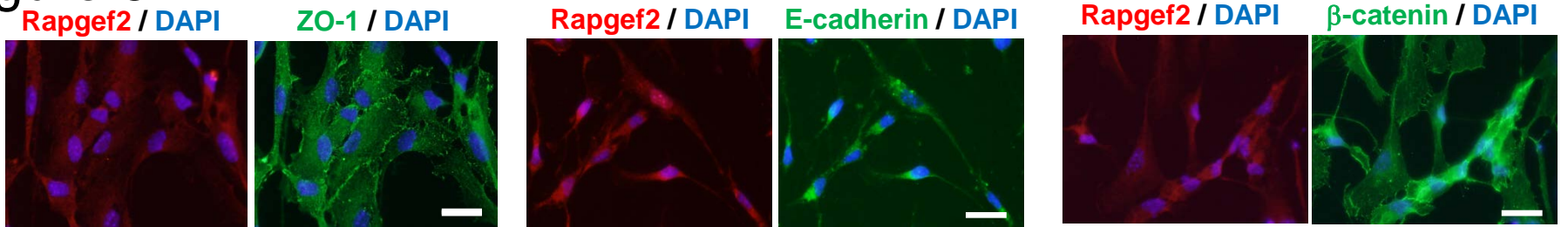


Supplementary Figure 2

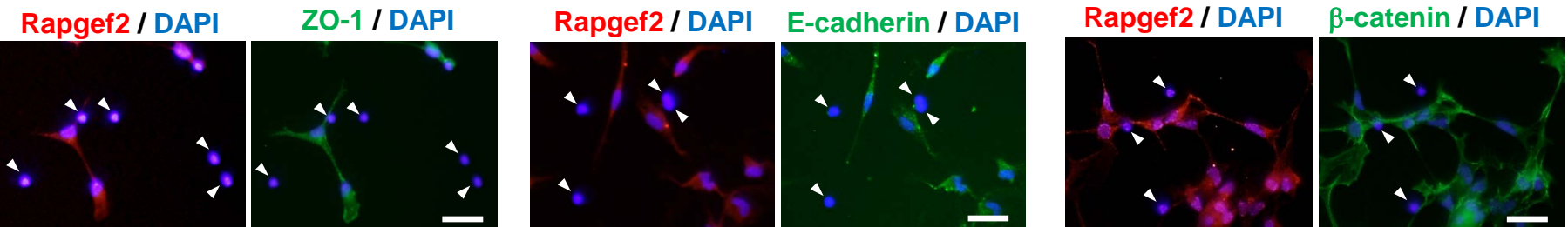


Supplementary Figure 3A

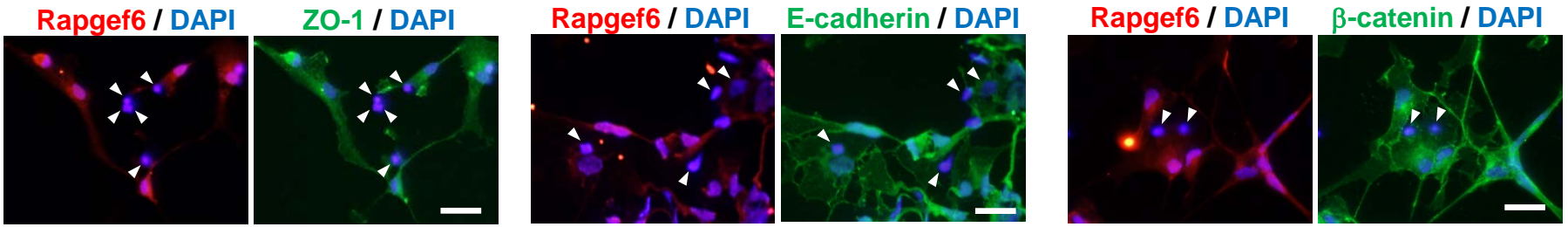
scramble RNA



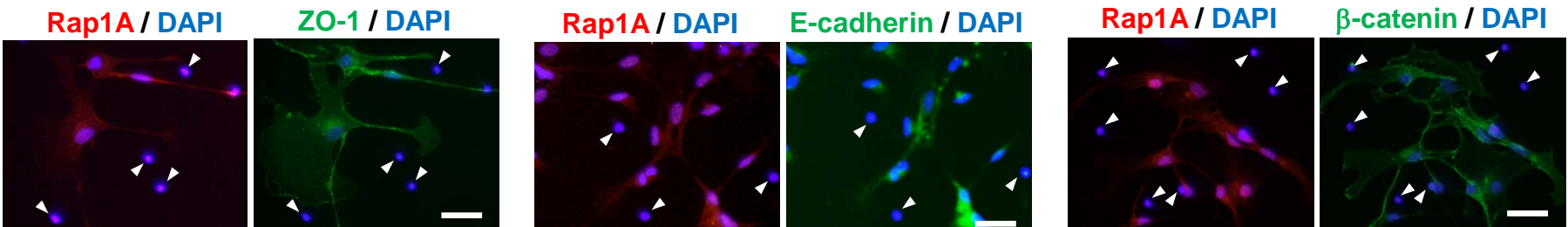
Rapgef2
siRNA



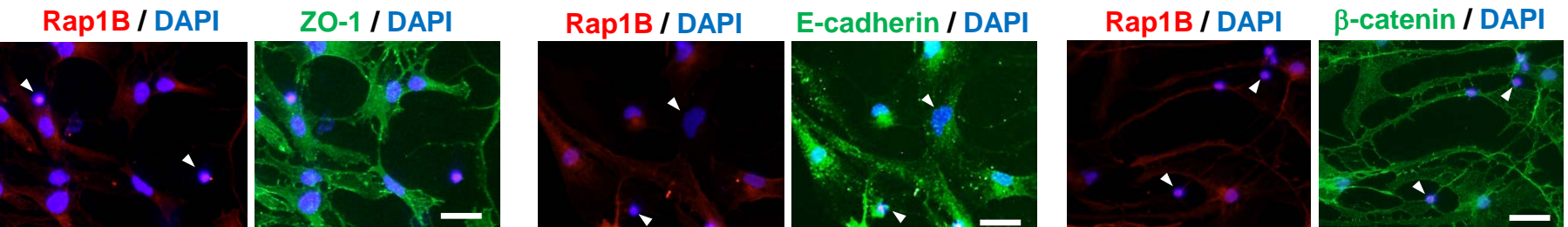
Rapgef6
siRNA



Rap1A
siRNA

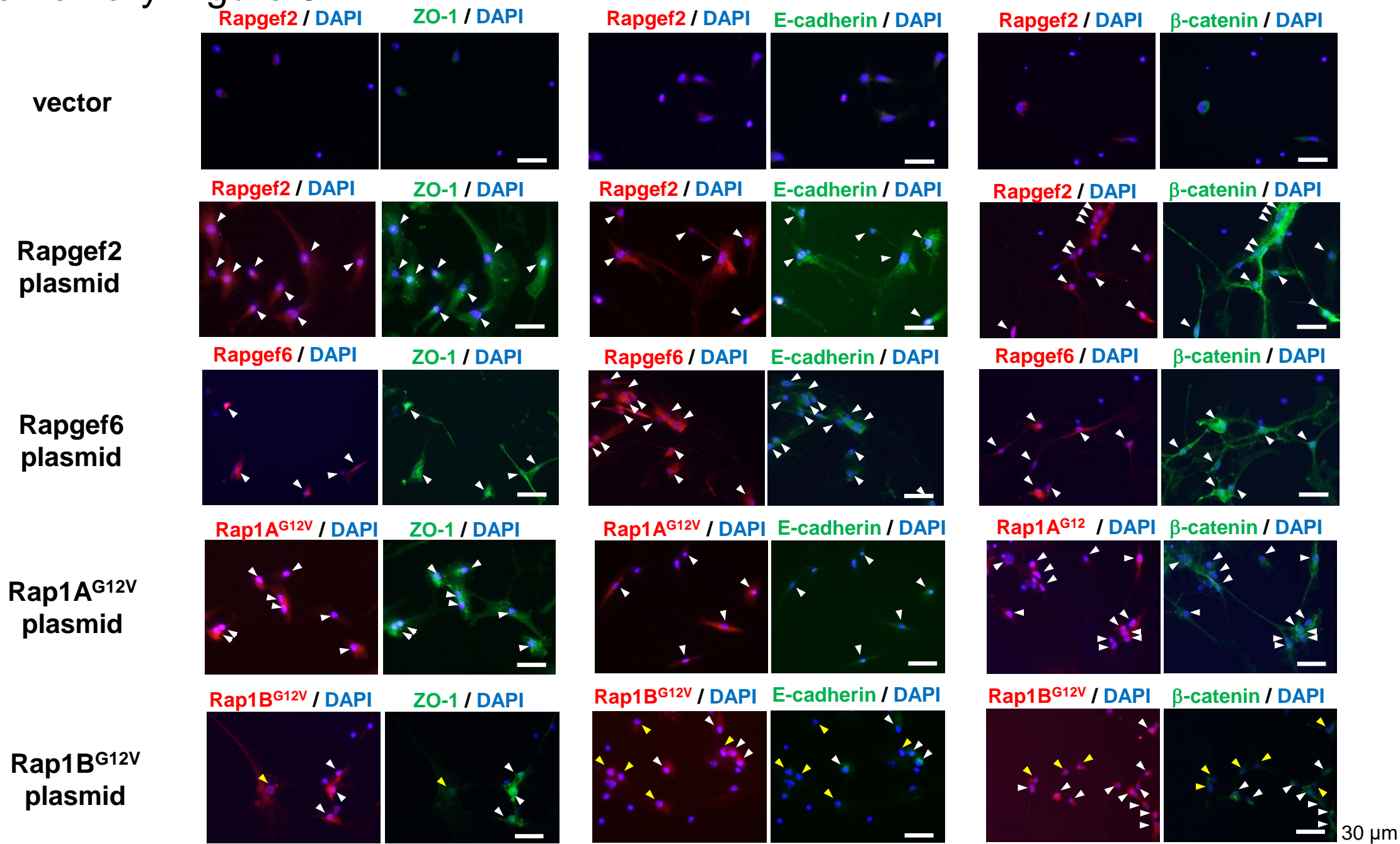


Rap1B
siRNA

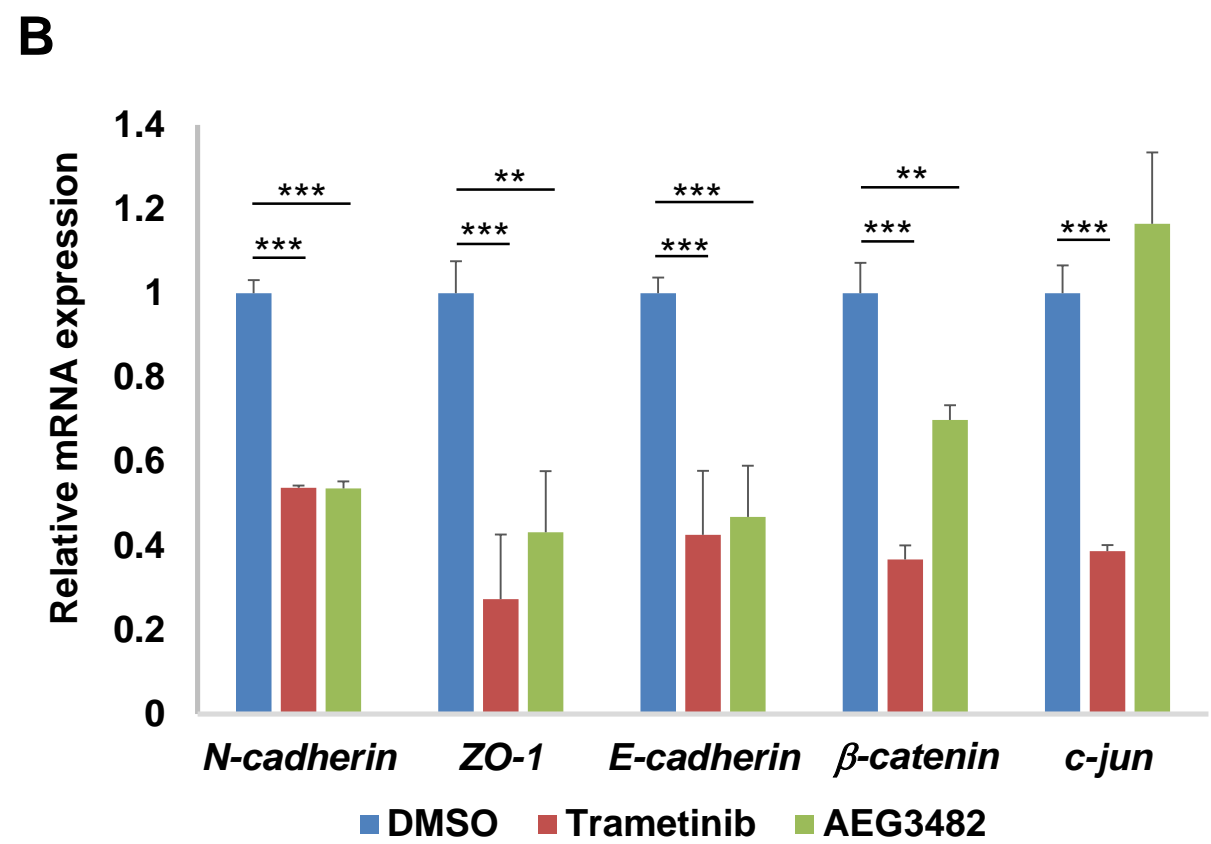
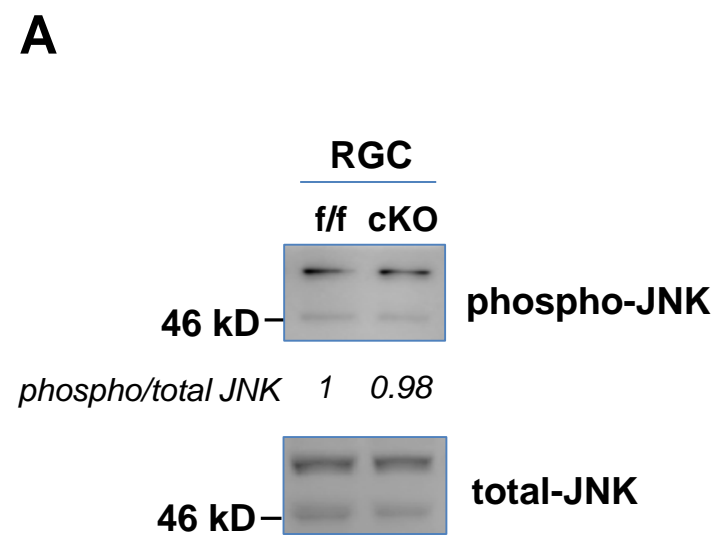


30 μ m

Supplementary Figure 3B



Supplementary Figure 4



Supplementary Table 1. Primers used for qRT-PCR

Gene of interest	Sense	Anti-sense
<i>Rapgef2</i>	5'-tcaacatggaccctgccctta-3'	5'-ccgcctgtctgagcaacatc-3'
<i>Rapgef6</i>	5'-cagcacctgccaagactgtca-3'	5'-cttgctgtaagcagtggctgga-3'
<i>Rap1A</i>	5'-gccaaagggttgcactagtttattc-3'	5'-tttgccaactacccgttcac-3'
<i>Rap1B</i>	5'-ctcgtcgtgcttggatcagg-3'	5'-gcatacactgctgtgcatctacttc-3'
<i>β-catenin</i>	5'-cgccgcttataaatcgctcc-3'	5'-caggtcagcttgagtagcca-3'
<i>ZO-1</i>	5'-gagcaggcttggaggagac-3'	5'-cattgctgtgctcttagcgg-3'
<i>E-cadherin</i>	5'-cgccacagatgatggttcac-3'	5'-ggttatccgcgagcttgaga-3'
<i>N-cadherin</i>	5'-agggtggacgtcattgtagc-3'	5'-ctgttgggggtctgtcagg-3'
<i>Afadin</i>	5'-cctgctgtctactactaccgataccgc-3'	5'-ccttctccctgggcttagctctac-3'
<i>c-jun</i>	5'-agcagggacccatggaagtt-3'	5'-aaagatgaccttgcttgtgcat-3'
<i>c-Fos</i>	5'-agaatccgaagggaagga-3'	5'-attgagaagaggcagggtga-3'
<i>β-Actin</i>	5'-atgaagatcaagatcattgctcctc-3'	5'-acatctgctggaaggtggacag-3'

Legends to Supplementary Figures

Fig. S1. Expression of the RGC markers. Passage 5 RGC cultures derived from *Rapgef2*-f/f (*f/f*) and *Rapgef2*-cKO (*cKO*) cerebral cortices were subjected to immunofluorescent staining with the anti-BLBP Ab (*upper panels*) (*red*) or the anti-nestin Ab (*lower panels*) (*red*). Nuclei were stained by DAPI (*blue*).

Fig. S2. Reduction of the AJ protein expression in *Rapgef2*-deficient neurospheres. Lysates of passage-5 neurosphere cultures derived from *Rapgef2*-f/f (*f/f*) and *Rapgef2*-cKO (*cKO*) cerebral cortices were subjected to the detection of the indicated proteins by western immunoblotting with the respective Abs. The numbers below the lanes indicate the relative band intensities of the respective proteins normalized by those of β -actin.

Fig. S3. Effect of knockdown and overexpression of *Rapgef2*, *Rapgef6*, *Rap1* on AJ protein expression. (A) The *Rapgef2*-f/f RGC cultures described in Fig. 3A were subjected to double immunofluorescence staining with the anti-*Rapgef2* Ab (*red*) and either of anti-ZO-1, anti-E-cadherin or anti- β -catenin Ab (*green*). Nuclei were stained by DAPI (*blue*). White arrowheads indicate the cells in which expression of the respective protein was substantially reduced compared to the scramble RNA-transfected cells. (B) The *Rapgef2*-cKO RGC cultures described in Fig. 3C were subjected to double immunofluorescence staining with the anti-*Rapgef2* Ab (*red*) and either of anti-ZO-1, anti-E-cadherin or anti- β -catenin Ab (*green*). Nuclei were stained by DAPI (*blue*). White arrowheads indicate the cells which showed higher

expression of the respective protein compared to the vector-transfected cells. Yellow arrowheads indicate the cells which failed to show higher expression of the respective protein while overexpressing Rap1B.

Fig. S4. Roles of ERK and c-jun in Rapgef2/Rap1A-dependent regulation of AJ protein expression. (A) Lysates of the RGC cultures described in in Fig. 2A were subjected to the detection of total and phosphorylated JNK by western immunoblotting with the respective Abs. The numbers below the lanes indicate the relative values of the phosphorylated JNK/total JNK. (B) The *Rapgef2*-f/f RGC cultures treated with DMSO, Trametinib or AGE3482 as described in Fig. 4C (A) were subjected to the measurements of the indicated mRNA levels by qRT-PCR. The data represent the mean \pm SEM of the results of 3 independent experiments, each conducted in quadruplicate.